Aggregation of Stilbene Derivatized Fatty Acids and Phospholipids in Monolayers and Vesicles[1]

Xuedong Song,[†] Cristina Geiger, Mohammad Farahat, Jerry Perlstein, and David G. Whitten*,[‡]

Contribution from the Department of Chemistry and NSF Center for Photoinduced Charge Transfer, University of Rochester, Rochester, New York 14627

Received July 10, 1997[⊗]

Abstract: Synthetic fatty acid and phosphatidylcholine amphiphiles incorporating a *trans*-stilbene (TS) chromophore in the fatty acid chain have been found to exhibit sharp changes in absorption and fluorescence spectra upon self-assembly in Langmuir−Blodgett films and aqueous dispersions. The spectral changes are readily associated with aggregates in which there is a strong noncovalent interaction between the TS chromophores. In this paper, we report determination of the size, structure, and properties of these "supramolecular" aggregates using both experiments and simulations. Important findings are that the key "unit aggregate" having distinctive spectroscopic properties is a cyclic "pinwheel" tetramer characterized by strong edge−face interactions. These tetramers may be packed together to form an extended aggregate with only small changes in absorption or fluorescence properties. While it was initially expected that aggregation occurred as a consequence of amphiphile self-assembly, studies of films of the stilbene fatty acids at the air−water interface show the predominance of aggregate prior to compression. Similarly in phospholipid dispersions aggregates persist above temperature at which chain melting occurs. Aggregation produces strong effects on the photophysics and photochemistry of the TS chromophore. No photoisomerization occurs; however, a slow photobleaching is observed for certain assemblies which can be attributed to formation of a photodimer. Fluorescence from aggregated TS chromophores is attributed to extended aggregates and dimers (excimers), and the latter is likely responsible for the photodimerization. The supramolecular aggregates observed in this study appear quite general and closely related to those observed with a wide variety of amphiphiles incorporating aromatic chromophores.

Introduction

Aggregation of *trans*-stilbene (TS, either simple[2−4] or polar substituted[5−7]) amphiphiles, especially, *trans*-stilbene fatty acid derivatives (SFAs, see Chart 1) in monolayers and Langmuir−Blodgett (LB) films has been observed in several investigations. While these compounds can be dispersed in micelles or saturated phospholipid vesicles at high dilution to give absorption and fluorescence similar to that observed for the same compounds in dilute organic solutions, their photophysical behavior in either pure or mixed (with saturated fatty acids such as arachidic acid) supported Langmuir−Blodgett (LB) films is quite different.[4] In many cases, SFAs form stable monolayers at the water−air interface which can be transferred onto solid substrates to form LB films.[2] The monolayers and LB films of SFAs exhibit blue-shifted absorption and red-shifted fluorescence relative to the spectra in organic solvents. This type of spectral shift has been attributed to the formation of H-aggregates in which the chromophores stack in a "card-pack" array.[2] Since the SFAs exhibit film-forming properties (isotherms, limiting area/ molecule, etc.)[4] very similar to linear saturated fatty acids such as arachidate, the formation of a card-pack aggregate was

Chart 1

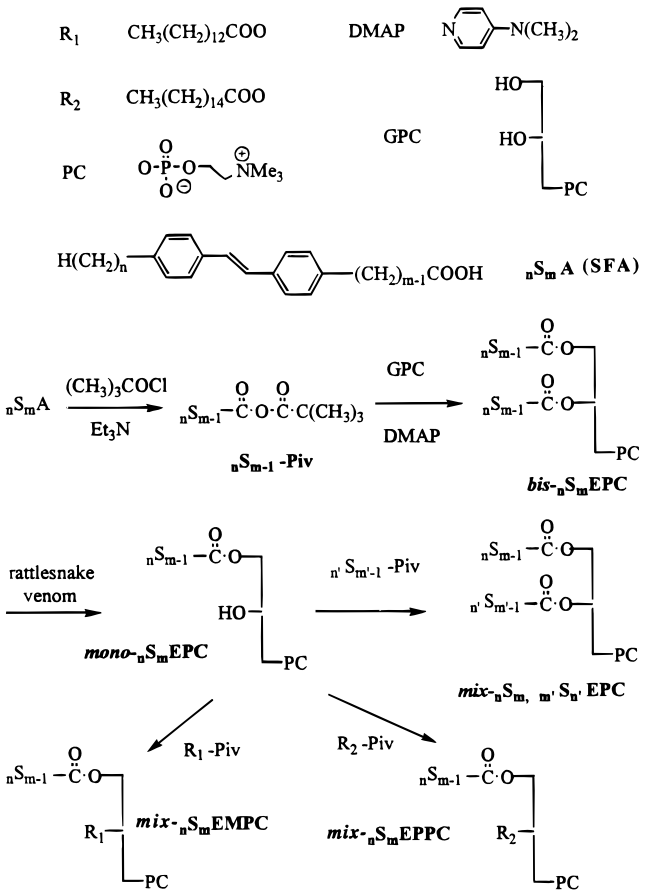

[†] Current address: CST-1, Los Alamos National Laboratory, Los Alamos, NM 87545.

[⊗] Abstract published in *Advance ACS Abstracts,* December 1, 1997.

(1) A portion of this research has appeared in preliminary communications. (a) Song, X.; Geiger, C.; Furman, I.; Whitten, D. G. *J. Am. Chem. Soc.* **1994**, *116*, 4103. (b) Song, X.; Geiger, C.; Leinhos, U.; Perlstein, J.; Whitten, D. G. *J. Am. Chem. Soc.* **1994**, *116*, 10340.

(2) Whitten, D. G. *Acc. Chem. Res.* **1993**, *26*, 502.

(3) Spooner, S. P.; Whitten, D. G. *Proc. SPTE Int. Soc. Opt. Eng.* **1995**, *117*, 7816.

(4) Mooney, W. F., III.; Brown, P. E.; Russell, J. C.; Costa, S. B.; Pedersen, L. G.; Whitten, D. G. *J. Am. Chem. Soc.* **1984**, *106*, 5659.

(5) Furman, I.; Geiger, H. C.; Whitten, D. G.; Penner, T. L.; Ulman, A. *Langmuir* **1994**, *10*, 837.

(6) Lippitsch, M. E.; Draxler, S.; Koller, E. *Thin Solid Films* **1992**, *217*, 162.

(7) Breton, H. L.; Letard, J. F.; Lapovyade, R.; Lecalvez, A.; Rassoul, R. M.; Freysz, E.; Ducasse, A.; Belin, C.; Morand, J. P. *J. Phys. Lett.* **1995**, *242*, 604−616.

S0002-7863(97)02292-0 CCC: $14.00

initially assumed to be a consequence of forcing the chromophores together in the process of forming the solid LB films at the air−water interface. A surprising finding was that the aggregates of SFAs on monolayers and LB films appeared resistant to dilution with saturated fatty acids such as arachidic acid.[8] The SFAs remain aggregated even when a relatively high ratio of saturated fatty acids was co-spread on the water surface such that on a statistical basis little aggregate should be expected.[2,8] These results suggest that the aggregation process for the SFAs must be energetically favorable in order to overcome the decrease in entropy caused by aggregation. This observation is further supported by the finding that mixtures of different SFAs in monolayers and LB films form H-aggregates similar to those for pure SFA monolayers and LB films with no evidence of the occurrence of any mixed aggregates.[8] All of these observations suggested that aggregation of the SFAs in LB films is a more complex process than initially suspected and that the aggregates might be more stable and more complex than a simple sandwich or card-pack as might be proposed from simple packing considerations.[2] In LB films, an apparent phase separation occurs in which SFAs form small stable aggregate clusters separated by matrices of the saturated fatty acid. Since the hydrophobicity of SFAs and saturated fatty acids used for the dilution are similar, the energy stabilizing the clusters is attributed to noncovalent interactions between stilbenes, which must be stronger than simple hydrophobic interaction between hydrophobic chains. This phenomenon is also observed for related aromatic compounds such as 1,4-diphenyl-1,3-butadiene,[8] 1,6-diphenyl-1,3,5-hexatriene,[8] azobenzene,[9] and squaraine derivatives.[10]

From the results obtained from supported multilayers and LB films of SFAs at the air−water interfaces, important questions related to chromophore aggregation emerge: what is the aggregate structure on a molecular level and what is the nature of the stabilization of these aggregates? Since direct probing of aggregate structures is extremely difficult, we have applied several indirect approaches including spectroscopies, conventional solution techniques, and Mount Carlo simulations to obtain information about the aggregate structures. The difficulty in manipulating LB films and monolayers, led us to study the aggregation in aqueous dispersions because of the experimental convenience and expected structural similarities among bilayer vesicles, monolayers, and LB films. We have designed and synthesized several stilbene-derivatized phospholipids (SPLs) which were anticipated to form bilayer assemblies in aqueous solution. It was found that the aggregates formed in aqueous SPL assemblies show similar spectroscopic behavior to those formed in the monolayers and LB films of SFAs. In this paper, we discuss the determination of the size and structure of the aggregates formed from the SPLs as well as their photophysics. Results of our study based on experiments and simulation indicate that the key stilbene "unit aggregates" are small and relatively stable, chiral "pinwheel" structures stabilized by strong noncovalent interactions.

Experimental Section

(A) Materials and General Techniques. Synthetic reagents were purchased from Aldrich Chemical Company and used as received unless otherwise stated. α-, *β*-, and *γ*-Cyclodextrins (CDNs, 99+%) were purchased from Aldrich. Rattlesnake venom, L-α-glycero-3-phosphorylcholine as the cadmium chloride complex, lipophilic Sephadex LH-20 (25−100 *μ*m bead), Sephadex-50G, L-α-dimyristoylphosphatidylcholine (DMPC, 99+%) and L-α-dipalmitoylphosphatidylcholine (DPPC, 99%) were obtained from Sigma Chemical Company. All solvents for spectroscopic studies were spectroscopic grade from Fisher or Aldrich. Milli-Q water was obtained by passing in-house distilled water through a Millipore-RO/UF water purification system. Deuterated solvents were purchased from MSD Isotopes or Cambridge Isotope laboratories. 3-(4-Methylbenzoyl)propionic acid was obtained from Lancaster. 4-(*N*,*N*-Dimethylamino)pyridine (DMAP), recrystallized from chloroform/diethyl ether, and trimethylacetyl chloride were purchased from Aldrich. Rexyn I-300, mixed resin, is from Fisher Scientific.

Melting points were taken on an El-Temp II melting point apparatus and are uncorrected. Proton NMR spectra were recorded on a General Electric QE300 MHz spectrometer using deuterated solvent locks or on a 500 MHz Varian VXR-500S spectrometer; coupling constants (*J*) are reported in hertz. FAB mass spectra were measured at the Midwest Center for Mass Spectrometry. Absorption spectra were obtained on a Hewlett-Packard 8452A diode array spectrophotometer. The circular dichroism (CD) study was carried out on a JASCO J-710 spectropolarimeter. Fluorescence spectra were recorded on a SPEX Flurolog-2 spectrofluorimeter and were uncorrected. Fluorescence quantum yields (QY) were determined by comparison with a standard *trans*-stilbene in methylcyclohexane (QY = 0.05). Differential scanning calorimetry (DSC) measurements were carried out on a MC-2 Ultrasensitive scanning calorimeter from MicroCal, Inc. Size extrusion experiments for vesicles were performed with an extruder through CoStar nucleopore polycarbonate filters. Dynamic light scattering measurements were carried out at the Eastman Kodak Research Laboratories.[11] All samples were routinely filtered through a 1.2 *μ*m nylon syringe filter before data acquisition. Cryo-transmission electron microscope measurements (Cryo-TEM) were made at the laboratory of NSF Center for Interfacial Engineering, Department of Chemical Engineering, University of Minnesota.[12] Specific wavelengths for irradiation were obtained from a 200 W Mercury/Xenon lamp (Oriel) through a monochromator (10 nm slit).

The general methods used for preparing Langmuir−Blodgett films and self-assemblies are based on techniques described by Kuhn et al.[13] Monolayers of SFAs or SPLs were prepared by spreading a chloroform solution of the material to be studied onto an aqueous subphase containing cadmium chloride (2.5×10^{-4} M) and sodium bicarbonate (3×10^{-5} M, pH = 6.6−6.8) on a KSV 5000 automatic film balance at room temperature (23 °C). The monolayers were then transferred onto quartz substrates. Reflectance spectra for monolayers at the air−water interface were recorded with a SD1000 fiber optics spectrometer (Ocean Optics, Inc.) equipped with optical fibers, an LS-1 miniature tungsten halogen lamp, and a CCD detector. Bilayer vesicles were prepared according to established protocols (all of the bilayer dispersions were prepared by sonication).[14] A cell disrupter W220F from Heat Systems Ultrasonics, Inc. (setting 6.5, 35 w) was used for probe-sonication. Aggregate size measurements and sample preparation for Cryo-TEM are identical to the procedures[9] reported for azobenzene derivatized phospholipids (APLs).

(B) Fluorescence Lifetime Measurements. Time-correlated single photon counting experiments were carried out on an instrument consisting of a mode-locked Nd:YLF laser (Quantronix) operating at 76 MHz as the primary laser source. The second harmonic (KTP crystal) of the Nd:YLF laser was used to synchronously pump a dye laser (Coherent 700) circulating Rhodamine 6G in ethylene glycol as the gain medium. The pulse width of the dye laser was typically 8 ps, as determined by autocorrelation, and was cavity dumped at a rate of 1.9 MHz. The desired excitation wavelength (295 nm) was obtained by frequency doubling of the dye laser output in a BBQ crystal. Emission from the sample was collected by two convex lenses and

(8) Spooner, S. P. Ph.D. Dissertation, University of Rochester, 1993.

(9) (a) Song, X.; Perlstein, J.; Whitten, D. G. *J. Am. Chem. Soc*. **1995**, 117, 7816. (b) Song, X.; Perlstein, J.; Whitten, D. G. *J. Am. Chem. Soc*. **1997**, *119*, 9144.

(10) (a) Chen, H.; Law, K. Y.; Whitten, D. G. *J. Am. Chem. Soc*. **1995**, *117*, 7257. (b) Chen, H.; Farahat, M. S.; Law, K. Y.; Perlstein, J.; Whitten, D. G. *J. Am. Chem. Soc*. **1996**, *118*, 2586.

(11) Light scattering studies were performed by Dr. Thomas Whitesides of the Eastman Kodak Research Laboratories.

(12) The cryo-TEM measurements were carried out in the Department of Chemical Engineering, University of Minnesota, with assistance of Dr. Michael Bench.

(13) Kuhn, H.; Môbius, D.; Böcher, H. In *Physical Methods of Chemistry*; Weissberger, A., Rossiter, B. W., Eds.; Wiley: New York, 1972; Vol. 1, p 577.

(14) (a) Hope, M. J.; Bally, M. B.; Webb, G.; Cullis, P. R. *Biophys. Acta* **1985**, *55*, 812. (b) Saunders, L.; Perrin, J.; Gammock, D. B. *J. Pharm. Pharmacol*. **1962**, *14*, 567.

focused at the entrance slit of a Spex 1681 monochromator (0.22m) and was detected by a multichannel plate (MCP) detector (Hamamtsu R3809U-01). The single photon pulses from the MCP detector were amplified and used as the stop signal for a time to amplitude converter (TCA, EG&G Ortec) while the signal from a photodiode, detecting a small fraction of the dye laser output, was used as the starting signal for the TCA. The starting and stop signals for the TCA were conditioned before entering the TCA by passing through two separate channels of a constant fraction discriminator (CFD, Tennelec). The output of the TCA was connected to a multichannel analyzer (MCA) interface board (Norland 5000) installed inside a 486DX2 personal computer. The MCA was controlled by software from Edinburgh Instruments (Edinburgh, U.K.). The same software was used to carry out the deconvolution of the data and exponential fitting using a nonlinear least-squares method. Measurements were made with air-saturated samples.

(C) Synthesis. The nomenclature and synthetic schemes used for preparation of the SPLs in this study are shown in Chart 1. The general synthetic approach is based on methods previously described in the literature.[15] These SPLs spontaneously form bilayer assemblies in aqueous solutions as do their natural counterparts such as DPPC and DMPC. For comparison, *mono*-SPLs were designed to prevent the formation of extended chromophore aggregates. The mixed *bis*-SPLs were originally expected to facilitate the formation of J-aggregates through the mismatch of the stilbenes in the two fatty acid chains. Instead, H-aggregates are exclusively formed.

***bis*-$_4$S$_6$EPC.** $_4$S$_6$A (0.44 mmol, 1.0 equiv) was dissolved in methylene chloride (20 mg/mL) and dry triethylamine (2.0 equiv) was added via syringe, followed by trimethylacetyl chloride (Piv-Cl, 4.0 equiv). TLC (solvent B, $CHCl_3$/methanol/water = 65/25/4) showed that the reaction was complete after ca. 5 h of stirring. After the solvent was removed with a stream of nitrogen, the residue was dried in a vaccum dessicator for 2 h and then dissolved in methylene chloride (20 mg/mL), followed by addition of a suspension of L-α-glycero-3-phosphorylcholine as the cadmium chloride complex (GPC·$CdCl_2$, 1.0 equiv) and 4-(*N*,*N*-dimethylamino)pyridine (DMAP, 2.0 equiv) in 2 mL of methylene chloride. The reaction mixture was stirred at room temperature for ca. 48 h. The solvent was removed by rotary evaporation, and the residue was dissolved in solvent A (methanol/chloroform/water = 5/4/1). The solution was filtered and passed through an ion exchange column, Rexyn-I 300, to remove the $CdCl_2$ and DMAP using solvent B as eluent. After the solvent was removed, the crude product was purified by passing it through a sephadex LH-20 column eluted with chloroform followed by recrystallization with chloroform/ether. Yield: 45%; mp = 228−234 °C. ^{1}H NMR ($CDCl_3$) δSPCLN 0.92 (t, 6H), 1.36 (m, 8H), 1.61 (m, 12H), 2.30 (m, 4H), 2.61 (m, 8H), 3.36 (s, 9H), 3.73−4.48 (m, 8H), 5.23 (m, 1H), 7.0−7.5 (m, 20H). FAB: *m*/*z* calcd for $[M + H]^+$ = 922.5, found 922.5.

***bis*-S$_4$EPC.** The preparation procedure is identical to that for bis-$_4$S$_6$EPC. Yield: 51%. ^{1}H NMR (500 MHz, $CDCl_3$) δ: 7.49 (d, J = 7.5, 4H), 7.42 (dd, J = 7.5, 2.0, 4H), 7.35 (t, J = 7.5, 4H), 7.27 (overlap with peak of $CDCl_3$, 4H), 7.15 (dd, J = 7.0, 4.5, 4H), 7.06 (s, 4H), 5.25 (m, 1H), 4.38 (m, 3H), 4.16 (dd, J = 7.5, 5.0, 1H), 4.04 (t, J = 6.5, 2H), 3.85 (m, 2H), 3.32 (s, 9H), 2.62 (m, 4H), 2.34 (m, 4H), 1.92 (m, 4H). FAB: *m*/*z* calcd for $[M + H]^+$ = 754.3, found 754.3.

***bis*-$_4$S$_4$EPC.** The synthesis of this compound is identical to that for bis-$_4$S$_6$EPC. Yield: 46%; mp = 230−237 °C. ^{1}H NMR ($CDCl_3$) δSPCLN 0.95 (t, 6H), 1.38 (m, 4H), 1.61 (m, 4H), 1.96 (m, 4H), 2.34 (m, 4H), 2.64 (t, 8H), 3.30 (s, 9H), 3.64−4.50 (m, 8H), 5.26 (m, 1H), 7.0−7.5 (m, 20H). FAB: *m*/*z* calcd for $[M + 1]^+$ 866.4, found 866.4.

***bis*-S$_{10}$EPC.** The preparation procedure is identical to that for bis-$_4$S$_6$EPC. Yield: 84%; mp = 184−190 °C. ^{1}H NMR ($CDCl_3$) δ: 1.30 (m, 20H), 1.62 (m, 8H), 2.32 (t, 4H), 2.63 (t, 4H), 3.38 (s, 9H), 3.70−4.50 (m, 8H), 5.23 (m, 1H), 7.0−7.6 (m, 22H). FAB: *m*/*z* calcd for $[M + 1]^+$ = 922.5, found 922.5.

***bis*-S$_6$EPC.** The sythesis of this compound is identical to that for *bis*-$_4$S$_6$EPC. Yield: 42%; ^{1}H NMR ($CDCl_3$) δSPCLN 1.30−1.36 (m, 4H), 1.55−1.64 (m, 8H), 2.24−2.30 (t, 4H), 2.53−2.60 (t, 4H), 3.24−3.34 (s, 9H), 3.80−4.40 (m, 8H), 5.20 (brs, 1H), 7.00−7.50 (m, 22H). FAB: *m*/*z* calcd for $[M + 1]^+$ = 810.4, found 810.4.

***mix*-$_4$S$_6$,S$_{10}$EPC.** *bis*-$_4$S$_6$EPC (100 mg, 0.11 mmol) was dissolved in 20 mL of CH_2Cl_2/MeOH (99:1, v/v), followed by addition of 10 mL of an aqueous solution containing 20 mM Tris-HCl (pH 8.0), 40 mM $CaCl_2$, and 2 mg of rattlesnake venom (*Crotalus adamanteous*). The reaction vessel was stirred vigorously in the dark for 3 days. When the reaction was complete, the organic solvent was removed by a stream of nitrogen and the lyso product was extracted by the Bligh−Dyer procedure.[15d] The pure product was obtained by passing a Sephadex LH-20 column using chloroform as eluent. *mono*-$_4$S$_6$EPC was obtained in 65% yield. ^{1}H NMR ($CDCl_3$) δ: 0.86 (t, 3H), 1.32 (m, 4H), 1.56 (m, 6H), 2.28 (t, 2H), 2.55 (t, 4H), 3.14 (s, 9H), 3.46−4.28 (m, 10H). 6.95−7.4 (m, 10H).

mono-$_4$S$_6$EPC (39 mg, 1.0 equiv) of obtained above and DMAP (16 mg, 2.0 equiv) DMAP were dissolved in 3 mL of CH_2Cl_2, followed by addition of 66 mg of S$_{10}$-Piv (2.0 equiv) in 3 mL of CH_2Cl_2 prepared from S$_{10}$A and pivaloyl chloride (Piv-Cl). The reaction mixture was stirred at room temperature for 48 h. The solvent was then removed, and the product was extracted by the Bligh−Dyer procedure substituting 1 M HCl for water to remove the DMAP. The product was purified using a Sephadex LH-20 column with chloroform as eluent. Yield: 40%; mp = 164−182 °C. ^{1}H NMR ($CDCl_3$) δSPCLN 0.95 (t, 3H), 1.30 (m, 14H), 1.62 (m, 10H), 2.30 (t, 4H), 2.60 (m, 6H), 3.38 (s, 9H), 3.80−4.60 (m, 8H), 5.22, (m, 1H), 7.0−7.52 (m, 21H). FAB: *m*/*z* calcd for $[M + 1]^+$ = 922.5, found 922.5.

***mix*-$_4$S$_6$,S$_{12}$EPC.** The synthesis is identical to that for *mix*-$_4$S$_6$,S$_{10}$-EPC. Yield: 66%; mp = 260−268 °C. ^{1}H-NMR ($CDCl_3$) δ: 0.94 (t, 3H), 1.26 (s, 18H), 1.60 (m, 10H), 2.32 (s, 6H), 2.61 (m, 6H), 3.38 (s, 9H), 3.82−4.56 (m, 8H), 5.22 (m, 1H), 7.10−7.55 (m, 21H). FAB: *m*/*z* calcd for $[M + H]^+$ = 949.5, found 952.5.

***mix*-$_4$S$_6$EPPC.** The preparation procedure is similar to that for *mix*-$_4$S$_6$,S$_{10}$EPC. Yield: 44%; mp = 184−188 °C. ^{1}H NMR ($CDCl_3$) δSPCLN 0.86−0.99 (m, 6H), 1.26 (s, 24H), 1.34−1.72 (m, 12H), 2.25−2.66 (m, 8H), 3.43 (s, 9H), 4.0−4.60 (m, 8H), 5.24 (m, 1H), 7.0−7.5 (m, 10H). FAB: *m*/*z* calcd for $[M + H]^+$ = 828.5, found: 828.4.

***mix*-S$_4$EMPC.** The synthesis is similar to that for *mix*-$_4$S$_6$,S$_{10}$EPC. Yield: 51%. ^{1}H NMR (300 MHz, $CDCl_3$) δ: 0.90 (t, 3H), 1.24 (m, 18H), 1.56 (m, 2H), 1.93 (m, 2H), 2.28 (t, 2H), 2.36 (t, 2H), 2.65 (t, 2H), 3.32 (s, 9H), 3.68−4.44 (m, 8H), 5.23 (m, 1H), 7.06−7.54 (m, 11H). FAB: *m*/*z* calcd for $[M + H]^+$= 716.4, found 716.3.

Results and Discussion

All of the *trans*-stilbene (TS)-derivatized phospholipids (SPLs) including *bis*-SPLs, *mono*-SPLs, and *mix*-SPLs are readily soluble in organic solvents such as methylene chloride and chloroform to give solutions with absorption λ_{max} at 315 nm and fluorescence λ_{max} at 356 nm, which are characteristic of the TS monomer. The behavior is similar to that observed previously for SFAs in organic solvents.[2] The presence of normal "monomeric" absorption and fluorescence spectra for the SPLs suggests there is little or no tendency for the TS chromophores to associate in those solvents in either the ground or excited state, despite the close proximity of the chromophores in the phospholipids containing two TS units. The SPLs can be dispersed in water by probe sonication to form stable, clear aqueous solutions. In contrast to the "monomeric" spectra observed in organic solvents, the aqueous dispersions of SPLs show blue-shifted absorption and red-shifted fluorescence spectra which are attributed to the formation of TS H-aggregates similar to those observed in LB films[2] of SFAs and SPLs. To a first approximation the spectral shifts suggest the TS chromophores in the H-aggregates pack in a "card-pack" array where a new exciton band results from excitonic interaction between the transition dipole moments of the TS chromophores.[16] The only allowed transition for a "perfect" H-aggregate card-pack is to the highest energy level of the exciton band from the ground state, which results in a blue-shift in absorption spectra relative to the corresponding monomer. The presence of red-shifted fluorescence could be ascribed to emission from the

(15) (a) Kates, M. In *Methods in Membrane Biology* Korn, E. D., Ed.; Plenum: New York, 1977; Vol. 8, p 219. (b) Khorana, H. G.; Chakrabarti, P. *Biochemistry* 1975, *14*, 5021. (c) Bligh, E. G.; Dyer, W. J. *Can. J. Biochem. Physiol*. **1959**, *37*, 911.

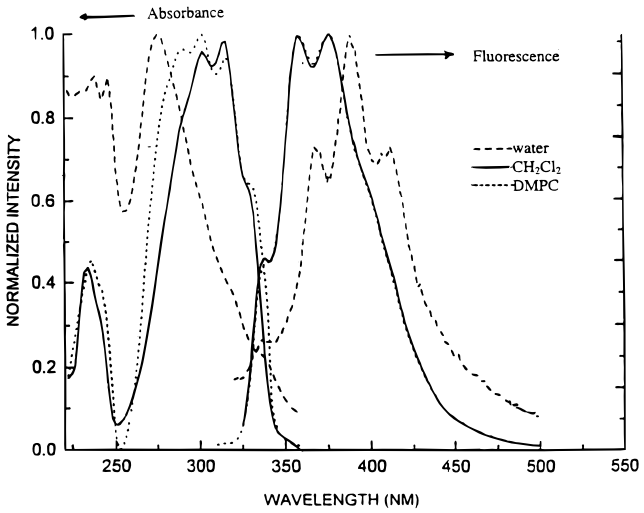

Figure 1. Absorption and fluorescence spectra of *bis*-S_{10}EPC in water, methylene chloride, and DMPC vesicles (DMPC/*bis*-S_{10}EPC = 100).

forbidden low-energy exciton band of the H-aggregates.[16] The SPLs can also be codispersed with an excess of the saturated phospholipids such as DPPC or DMPC in water to form mixed vesicles which exhibit absorption and fluorescence spectra similar to those of the monomers in organic solvents, but broader and less structured. The broader absorption spectra are assigned to a TS dimer on the bassis of the study of SFA and SPL complexes with cyclodextrins[45](CDNs, see below) as well as the results reported by others.[17,18] The broadening of the absorption spectrum can be ascribed to a small excitonic splitting for an oblique dimer.[35b] Although the absorption spectra of SPLs, in the presence of excess saturated phospholipid and SFA or SPLs in γ-CDN are similar, the fluorescence spectra are quite different with the latter showing a broad "excimer-like" fluorescence. Evidently, the restricted environment of DMPC and DPPC vesicles inhibits the formation of an TS excimer for SPLs while the two TS chromophores of SFAs or SPLs in γ-CDN are probably in a sufficiently flexible environment to adopt a geometry required for one excited TS to interact with another TS in the ground state to give the red-shifted excimer fluorescence. Compared to the broad absorption spectra of *bis*-SPLs in DPPC or DMPC, the absorption spectra of the *mono*-SPLs in the matrix of DPPC or DMPC vesicles are sharper, slightly red-shifted (4 nm) and with clear vibrational peaks similar to those of SFAs solubilized in DPPC and DMPC vesicles. The sharp fine-structured absorption spectra are associated with the TS monomer. The absorption and fluorescence spectra of *bis*-S_{10}EPC in water, CH_2Cl_2, and DMPC are shown in Figure 1, which are assigned to H-aggregate, monomer, and dimer, respectively. Since the spectrum in water is unaffected by dilution up to several-fold with DMPC, we attribute this spectrum to pure aggregate; similarly the spectrum in chloroform is identical to "monomer" alkylstilbene and thus attributed to pure monomer. The "dimer" spectrum in DMPC/water probably consists of a mixture of monomer, aggregate, and dimer, but the dimer predominates.

Although all SPL assemblies investigated in this paper show blue-shifted absorption and red-shifted fluorescence in water relative to the monomer in organic solvents, the precise extent of spectral shifts depends upon the structure of the individual molecule as shown in Table 1. Absorption spectra of *bis*-SPLs in water are always sharper and more blue-shifted than those for *mono*-SPLs, which have relatively broad spectra as indicated by their large full width at half maximum (FWHM). The broader, less blue-shifted absorption spectra of *mono*-SPLs are attributed to the perturbation of the saturated fatty acid chain, which should inhibit the formation of highly extended aggregates. The absorption spectra of *mix*-SPLs vary with their molecular structures. The absorption spectrum of *mix*-$_4S_6$,S_{10}-EPC, in which the two TS chromophores have a four-methylene offset, is particularly sharp with a large blue-shift in water relative to the monomer, while *mix*-$_4S_6$,S_{12}EPC, which has a six methylene group mismatch for the two TS chromophores, shows a broad absorption spectrum with a relatively small blue-shift. While the excitation spectrum of the monomer in an organic solution of SPL is identical to the corresponding absorption spectrum, excitation spectra of SPL assemblies in water are slightly different from their absorption spectra and show some emission wavelength dependence, particularly when monitored at the red edge of the fluorescence band. This is attributed to the microheterogeous nature of the bilayer system. The SPLs, moderately or highly diluted in DPPC or DMPC vesicles, display excitation spectra similar to their corresponding absorption spectra. As expected, they are also wavelength-dependent. SFAs and *mono*-SPLs in the presence of excess DMPC or DPPC show identical monomeric absorption and excitation spectra. The *bis*-SPLs in DPPC vesicles with a low dilution ratio of [DPPC]/[*bis*-SPL] (for example, 5) show excitation spectra intermediate between those of pure *bis*-SPL aggregates and TS monomer and exhibit emission wavelength-dependence. They can actually be fit into a summation of a mixture of dimers (or monomers in case of *mono*-SPLs) and H-aggregates.

Table 1. Absorption and Fluorescence Data for SPLs in Different Media

SPLs	chloroform (nm)		water (nm)		shift (nm)[d]		FWHM[b] (wn)[a]
	λ^{abs}_{max}	λ^{em}_{max}	λ^{abs}_{max}	λ^{em}_{max}	$\Delta\lambda^{abs}$	$\Delta\lambda^{em}$	
$_4S_6$A	315	356	268[c]	406[c]	47	50	
S_4EMPC	315	356	282	365	33	9	6340
$_4S_6$EPPC	315	356	282	391	33	35	6350
S_4EPC	315	356	276	423	39	67	4830
S_6EPC	315	356	270	395	45	39	4210
S_{10}EPC	316	358	273	389	43	33	4640
$_4S_4$EPC	320	360	274	417	41	61	4180
$_4S_6$EPC	320	366	274	400	41	44	3780
$_4S_6$, S_{10}EPC	318	365	272	418	44	62	6800
$_4S_6$, S_{12}EPC	286	366	278	420	37	64	6690

[a] Wavenumber. [b] Full width at half maximum. [c] Data in LB film on quartz. [d] Relative to $_4S_6$A in chloroform.

The absorption and fluorescence spectra for *bis*-S_4EPC and *bis*-S_6EPC assemblies in water persist over a broad range of temperatures from 5−80 °C with the exception of a gradual decrease in fluorescence intensity. This implies that the TS chromophores in the aggregates experience little change in packing geometry even at temperatures above T_c values at which the polymethylene chains melt. The persistence of the aggregates above chain-melting reinforces the idea of a relatively high stability for the TS aggregates and is supported by the observation that the H-aggregates in the monolayers and LB films of SFAs resist relatively high dilution with saturated fatty acids.[16]

Fluorescence. The fluorescence spectra associated with SPL assemblies in water are relatively complicated and can be assigned as due primarily to two different species: an aggregate and an excimer.[24] The aggregate has a higher fluorescence quantum yield (QY) and a lifetime of 3−10 ns, while the excimer has a lower fluorescence QY and a lifetime that is

(16) (a) Kasha, M. *Radiat. Res.* **1963**, *20*, 55. (b) Kasha, M.; Rawls, H. R.; El-Bayoumi, M. *Pure Appl. Chem.* **1965**, *11*, 371. (c) Hochstrasser, R. M.; Kasha, M. *Photochem. Photobiol.* **1964**, *3*, 317.

(17) Lewis, F. D.; Wu, T.; Burch, E. L.; Bassani, D. M.; Yang, J.; Schneider, S.; Jager, W.; Letsinger, R. L. *J. Am. Chem. Soc.* **1995**, *117*, 8785−8792.

(18) Anger, I.; Sandros, K.; Sundahl, M.; Wennerstrom, O. *J. Phys. Chem.* **1993**, *97*, 1920−1923.

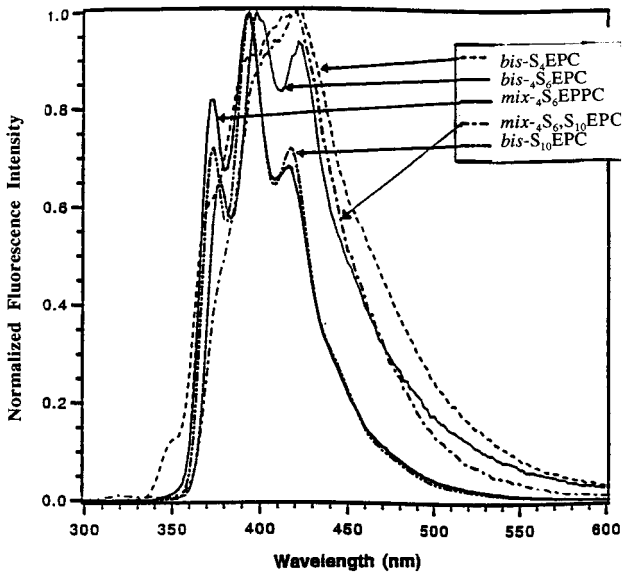

Figure 2. Comparism of fluorescence spectra of SPL assemblies in water, excited at 270 nm.

Table 2. Fluorescence Lifetimes and Quantum Yields for SPLs in Water

phospholipid	τ_3 (ns)[a]	τ_4 (ns)[a]	ϕ_f
mix-S_4EMPC	2.7 (91%)[b]	23.3 (9%)	
bis-S_4EPC	3.4 (13%)	22.6 (87%)	0.10
bis-S_6EPC	2.7 (35%)	18.5 (64%)	
bis-S_{10}EPC	3.2 (74%)	17.8 (26%)	0.74
DPPC/*bis*-S_{10}EPC[c]	3.4 (10%)	18.1 (90%)	
bis-$_4S_6$EPC	4.1 (52%)	15.9 (42%)	0.09
mix-$_4S_6$EPPC			0.43
mix-$_4S_6$,S_{10}EPC			0.10
bis-$_4S_4$EPC			0.10

[a] The data were obtained from time resolved fluorescence decay curves at 500 nm emission wavelength. [b] Values in parenthesis are contributions of the various decays to the total fluorescence intensity. [c] DPPC/S_{10}EPC = 110.

longer than 10 ns. The lifetimes for both species are longer than the radiative lifetime for TS (1.7 ns[43]). The variations in the excited state properties for the present systems originate from the differences in the structures of the molecules despite the presence of TS in all molecules as the photophysically active chromophore in the spectral region of interest. Figure 2 compares the fluorescence spectra of SPL assemblies in water. The fluorescence spectrum of *bis*-S_4EPC, as well as that of *mix*-$_4S_6$,S_{10}EPC, is broad and structureless with a large red-shift and low fluorescence QY (Table 2), which is attributed to an excimer type fluorescence, consistent with its structureless appearance and the low fluorescence efficiency. In contrast, *bis*-S_{10}EPC and *bis*-$_4S_6$EPPC assemblies give sharper, fine-structured, and relatively less red-shifted fluorescence with relatively high fluorescence QY, which is assigned to the aggregate. These two extreme cases of fluorescence spectra show insignificant excitation wavelength dependence. Several other SPLs such as *bis*-$_4S_6$EPC, *bis*-S_6EPC, and *mix*-S_4EMPC show intermediate fluorescence characteristic

The significant contribution of an excimer to the total fluorescence for several SPL assemblies can be rationalized by considering the two following possible mechanisms: (1) An energy transfer process from the major species, the aggregates, to residual dimers occurs in the systems. The small portion of dimers, which is not evident in the absorption spectra, can be, in some cases, a very efficient energy trap for the excitation created in the aggregates. Similar cases have been observed previously for both H- and J-aggregate systems[19−21] in organized assemblies. In fact, there is evidence for the formation of an excimer state for aromatic clusters that shows weak excitonic interaction in the ground state[22] (for this reason, the terms, dimer and excimer, are used interchangably in this paper). It appears that the structure of the SPL is responsible for the observed photophysical and photochemical (see photolysis section) variations. Both hydrophobic interaction of fatty acid chains and chromophore−chromophore interaction of TS play important roles in determining the aggregate structures. In a molecule such as *bis*-S_{10}EPC, where TS is situated relatively far away from the head group, the formation of highly ordered and uniform TS aggregates is favored probably due to the long fatty acid chains which are flexible enough to allow optimal geometry for the chromophore−chromophore interaction. Thus, the fluorescence originates mainly from the radiative decay of the excited states of the H-aggregates (unit aggregates). In contrast, the population of the dimer is expected to be relatively large for a molecule such as *bis*-S_4EPC in which the TS is close to the rigid head group. In this case, efficient energy transfer from the H-aggregates to the excimers occurs, and the fluorescence is generated directly from the TS excimer. Such efficient energy transfer from H-aggregates to excimers has also been observed for styrylthiophene[23] derivatives as well as for other systems.[19−21] In the cases of *bis*-$_4S_6$EPC, *bis*-S_6EPC, and *mix*-S_4EMPC, some energy transfer process occurs, which results in the intermediate fluorescence spectra. The dependence of the H-aggregation upon molecular structures has also been observed for azobenzene[9] and styrylthiophene derivatives.[23] (2) A variation in geometry after excitation to the excitonic state of the aggregate compared to the ground state geometry is responsible for the excimer fluorescence. In the case of *bis*-S_4EPC, due to the relatively small aggregate size, a small change in geometry is sufficient to allow excimer formation or even dimerization. The latter process is expected to be an inefficient process due to more demanding structural requirements for [2 + 2] cycloaddition in a restricted environment.[43] For *bis*-S_{10}EPC assemblies, the large, highly ordered and rigid aggregate appears to enhance the structural integrity of the TS aggregate to the point that even a small excited state structural change becomes unfeasible; therefore, excimer formation and photodimerization processes become inefficient.

Fluorescence Lifetime.[24] Due to the microheterogeous nature in SPL assemblies, a distribution of fluorescence lifetimes instead of discrete lifetimes are found.[24] The distribution f_i was characterized by its center lifetime τ_i, standard deviation σ_i and amplitude of the center lifetime A_i. The contribution of each lifetime distribution to the total fluorescence intensity at a given fluorescence wavelength can be estimated via eq 1.

$$f_i = \tau_i \sigma_i A_i / \sum_i \sigma_i \tau_i A_i \qquad (1)$$

The fluorescence lifetime (0.25 ns) and quantum yield (0.09) for *bis*-S_4EPC in methylene chloride are found to be similar to those for SFAs and simple TS in the same organic solvent.[2] However, the fluorescence decays of SPL assemblies in water are rather complicated and, in most of cases, can be fitted with four different lifetime distributions as shown in Figure 3 for *bis*-S_4EPC. The two short lifetimes for all SPLs are almost identical and center at τ_1 = 0.27 ns and τ_2 = 1.4 ns. Their

(19) (a) Evans, C. E.; Bohn, P. W. *J. Am. Chem. Soc.* **1993**, *115*, 3306. (b) Furman, I.; Whitten, D. G.; Penner, T. L.; Ulman, A. *Langmuir* **1994**, *10*, 837.
(20) Farahat, C. W.; Penner, T. P.; Ulman, A.; Whitten, D. G. *J. Phys. Chem.* **1996**, *100*, 12616.
(21) Kuhn, H. *J. Photochem.* **1979**, *10*, 111.
(22) Saigusa, H.; Lim, E. C. *J. Phys. Chem.* **1995**, *99*, 15738−15747.
(23) Song, X.; Perlstein, J.; Whitten, D. G. Submitted for publication.
(24) Whitten, D. G.; Farahat, M. S.; Gaillard, E. R. *Photochem. Photobiol.* **1997**, *55* (1), 23.

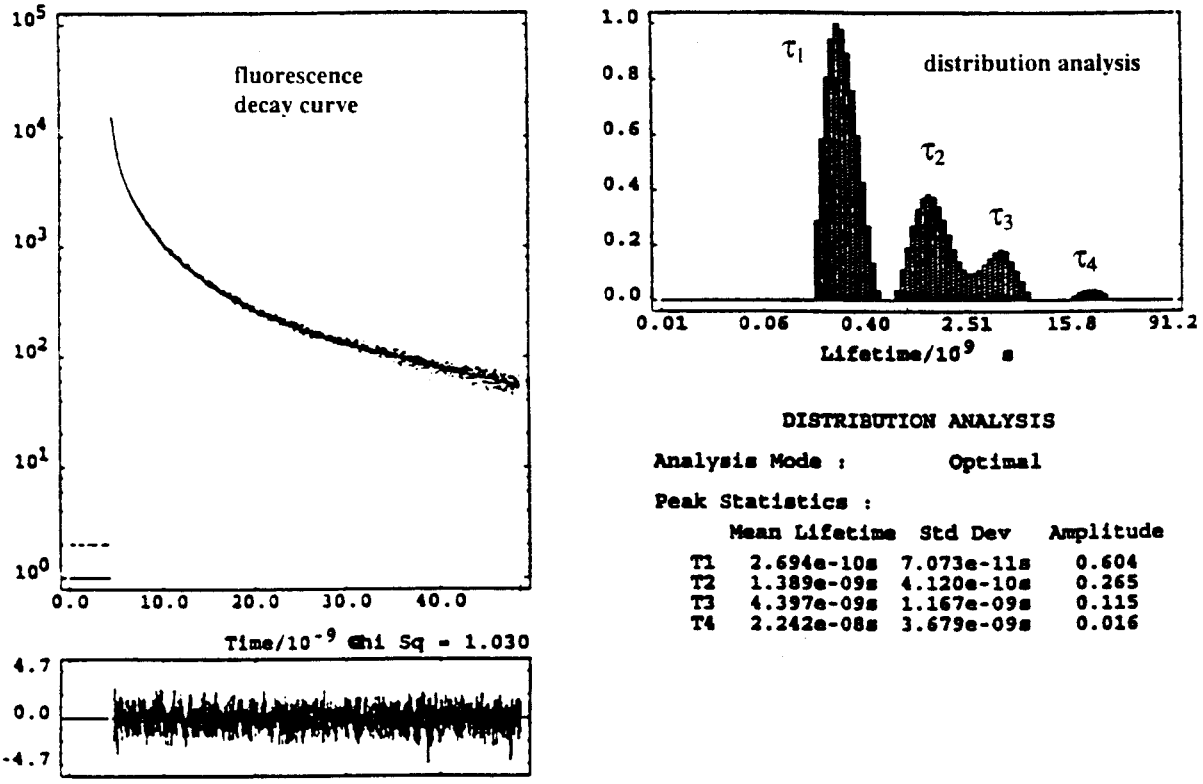

Figure 3. Fluorescence decay curve at 450 nm emission wavelength and lifetime distribution for *bis*-S_4EPC assemblies in water (excited at 300 nm).

fractional contributions to the total fluorescence are negligible (<5%). The shortest lifetime τ_1 is assigned to a nonconstrained TS monomer on the basis of its similar lifetime to that of $_4S_6A$ in CH_2Cl_2 (τ = 0.24 ns), and the negligible second shortest one τ_2 is attributed to a constrained TS monomer in the assemblies which is comparable to that of $_4S_6A$ in DPPC (1.8 ns) and in α-CDN (1.4 ns). The two long components, τ_3 and τ_4 are assigned to a TS H-aggregate and a TS excimer, respectively. The assignment of τ_4 to the TS excimer is based on the reported results for TS excimers (11 ns)[17] and our studies (see below) of SFAs in γ-CDN (5.3−17.6 ns).[18] The increase in lifetime for the H-aggregate relative to the monomer in organic solution is attributed mostly to the forbidden nature (symmetry)[16a] of the radiative transition from the lowest energy level of exciton band to ground state of H-aggregates as well as the restrictive matrices of vesicles which provide a large barrier for a competitive, nonradiative decay, namely, *trans*−*cis* isomerization. The contribution of the four emitting species to the total fluorescence intensity is fluorescence wavelength dependent for all SPLs. An increasing contribution of τ_1 can be detected at the blue-edge of the fluorescence whereas the major contributor at the peak of fluorescence is excimer. The lifetime data for other SPLs are summarized in Table 2 , which clearly indicate that both the total length of the aliphatic chains and the position of the TS chromophores in the aliphatic chains have effects on the characteristics of the fluorescence efficiency and lifetimes. The evidence for the above lifetime assignments also emerges from the dependence of the contribution of each lifetime on dilution by DPPC vesicles. While the contribution of two fast components change little with different dilution, the excimer component increases at the expense of the aggregate component when *bis*-S_{10}EPC is diluted in DPPC vesicles (DPPC/*bis*-S_{10}EPC = 110).

It is interesting to compare the contributions of the H-aggregate and excimer decays to the total fluorescence intensity for four *bis*-SPLs: *bis*-S_4EPC, *bis*-S_6EPC, *bis*-$_4S_6$EPC and *bis*-S_{10}EPC. There exists a clear consistency between the order of the aggregate and the relative contribution of the aggregats and excimer. For *bis*-S_4EPC assemblies where small aggregates are formed, the high contribution of excimer decay seems to support an efficient energy transfer from the H-aggregates to the excimers, while the fluorescence of *bis*-S_{10}EPC assemblies, where more uniform aggregates are expected, shows a relatively low contribution of the excimer.

Complexes with Cyclodextrins (CDNs). Solubility of several SFAs in water improves significantly in the presence of α-, β-, and γ-CDNs due to the formation of host−guest complexes.[25] The absorption spectrum (see the Supporting Information) of $_4S_6A$ complex with α-CDN is sharper than that with β-CDN, which exhibits an absorption spectrum similar to that for $_4S_6A$ in methylene chloride. The fluorescence spectra in α- and β-CDNs and methylene chloride are identical and are associated with TS monomer. The sharper spectrum in α-CDN suggests that the TS chromophore is probably close or even inside the hydrophobic cavity of α-CDN. In contrast, a broad absorption spectrum similar to that for SPLs highly diluted in DMPC or DPPC vesicles and a structureless, red-shifted fluorescence spectrum relative to the monomer are observed for $_4S_6A$ in γ-CDN, which are assigned to a TS dimer (or excimer). The absence of a red-shift for the fluorescence of SPLs in excess of DPPC or DMPC vesicles is probably due to the restricted environment, which prevents the formation of an excimer.[19] In most of cases, the fluorescence quantum yields (see the Supporting Information) of TSA's in α-, β- and γ-CDNs are higher than in CH_2Cl_2, due to the formation of the complexes which to some extent inhibits the photoisomerization of TS. The fluorescence decay of SFAs in α-CDN follows simple monoexponential decay while the fluorescence decays in β- and γ-CDNs are quite complicated and can be fit into either two or three components (see the Supporting Information). This suggests that in the latter cases, there exist more than one

(25) (a) Herkstroeter, W. G.; Martic, P. A.; Evans, T. R.; Farid, S. *J. Am. Chem. Soc.* **1986**, *108*, 3275. (b) Herkstroeter, W. G.; Martic, P. A.; Farid, S. *J. Am. Chem. Soc.* **1990**, *112*, 3583−3589.

emitting species in which the TS chromophores probably adopt different positions in the cavities of CDNs. In the case of γ-CDN, there may be both the monomer and the dimer. We suggest that an excimer or dimer is responsible for the long fluorescence lifetime in γ-CDNs, proposed to be an excimer. The long fluorescence lifetime for TS excimer has been reported previously by Lewis and co-workers.[17] The formation of the monomeric complexes of TSA's with α-, β-CDNs and a dimer in γ-CDN are further supported by the observation of moderate monophasic ICD spectra in α- and β-CDNs and biphasic ICD spectra in γ-CDN, which is characteristic of an oblique dimer (see the Supporting Information). The asymmetric feature of ICD in γ-CDN can be attributed to a mixture of both monomer and dimer in the solution as indicated by the broad fluorescence spectrum. Interestingly, the ICD signals for SFAs in all three CDNs disappear upon *trans*−*cis* photoisomerization of the TS, indicative of exclusion of the *cis*-stilbenes from the cavities of CDNs.

The tendency of self-aggregation for SPLs are much higher than the formation of inclusion complexes in aqueous solutions of α-, β-, and γ-CDNs. Addition of acetonitrile to the aqueous solutions favors the complexation over self-aggregation. The mixture of the aggregate, dimer, and monomer in a mixed solvent of acetonitrile/water (1/2) for SPLs can be converted into a monomer-dominating solution by addition of either α- or β-CDNs and a dimer-prevailing solution by addition of γ-CDN.

Characterization of SPL Assemblies. Three techniques dynamic light scattering, membrane extrusion, and cryo-transmission electron microscopy (Cryo-TEM), have been used to characterize SPL assemblies in water. Light-scattering data for aqueous dispersions of SPLs show a relatively narrow distribution of particle sizes (based on assumption of spherical particles), which are much larger than those formed from saturated phospholipids such as DPPC (*bis*-$_4$S$_4$EPC: 521 nm; *bis*-S$_4$EPC: 198 nm; *bis*-$_4$S$_4$EPC: 243 nm). The particle size for aqueous dispersions of *bis*-S$_4$EPC changes little from 10 to 55 °C. Incorporation of *bis*-$_4$S$_4$EPC in DPPC vesicles slightly increases the size of DPPC vesicles. Consistent with the results obtained from light scattering measurements, the self-assemblies of SPLs in water can not be extruded through a 100 nm polycarbonate membrane but can completely pass through a 2 μm membrane. The Cryo-TEM micrograph (Figure 4) of *bis*-S$_4$EPC assemblies in water shows rather interesting structures with two major morphologies: large open tubules covered with smaller pieces or fragments and small open-ended tubules. These are assumed to be bilayer structures. As expected from such open structures, the pure S$_4$EPC assemblies in water failed to trap any carboxyfluorescein (CF).[14,26]

Differential scaning calorimetry (DSC), dynamic light scattering, and fluorescence techniques were applied to investigate phase transition behaviors of SPL assemblies in water. No phase transition for *bis*-SPLs could be detected by DSC, possibly due to their low solubility in water (less than 1.5×10^{-4} M). Fluorescence spectroscopy provides a useful tool to study phase transitions of organized systems. The fluorescence spectra of SPL aggregates were found to persist within a wide range of temperatures from 5−80 °C with the exception of a decrease in intensity. The fluorescence intensity for SPL assemblies in water were found to show sharp decrease at certain temperatures (23 and 65 °C for *bis*-S$_4$EPC and *bis*-S$_6$EPC, respectively) at which phase transitions presumably occur. The light scattering intensity for *bis*-S$_4$EPC also shows a discontinuity at 23 °C, which is believed to be associated with a phase transition. DSC studies for the mixtures of SPL/DPPC show good solubilization of SPLs in DPPC vesicle hosts. The endothermic maxima for the mixtures of several SPLs with DPPC (SPL/DPPC = 1/100) are shifted to lower temperatures (1−2 °C) and are slightly broadened, compared to those for to pure DPPC vesicles (T_c = 42 °C). Such a decrease in T_c of DPPC vesicles is expected from the small perturbation caused by the incorporation of the foreign SPLs.

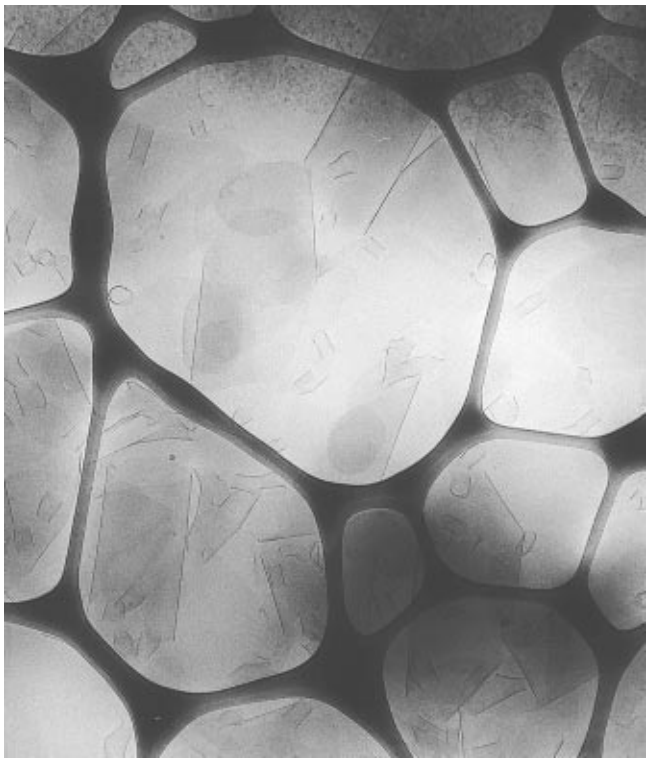

Figure 4. Cryo-TEM micrograph of *bis*-S$_4$EPC assemblies in water (3 days old, 2×10^{-4} M).

Aggregate Size. SPL assemblies in water undergo rapid mixing with DMPC or DPPC vesicles at or above T_c values of both microphases but only very slowly below T_c. We have reported previously[1] that a clean, simple conversion from the aggregates to dimers (monomers in the cases of *mono*-SPLs) occurs when SPL aggregates are mixed with DMPC or DPPC vesicles above T_c.[1] We also demonstrated that the aggregates and dimers or monomers in cases of *mono*-SPLs are two major species in the equilibrium solutions of SPLs moderately diluted in DPPC or DMPC vesicles. The equilibrium between the aggregates and dimers or monomers can be expressed by eq 2. Further evidence for the equilibrium emerges from the ICD spectra for the mixtures of DPPC or DMPC/SPLs with low dilution ratio from 5 to 35, which are identical to the ICD spectra of pure SPL assemblies in water (see below). A modified Benisi−Hildebrand approach[28] identical to the treatment of APLs (azobenzene-derivatized phospholipids)[9] and TPLs (styryl-thiophene-derivatized phospholipids)[23] is used to formulate the equilibrium, and eq 5 is obtained in terms of absorbance of the aggregates and dimers or monomers. The plot of ln A_{agg} versus ln[$A^o_{agg} - A_{agg}$] should give a straight line while the slope allows determination of the aggregate size, n, which is the number of SPL molecules per aggregate.

(26) (a) Weinstein, J. N.; Yoshikami, S.; Henkart, P.; Blumenthal, R.; Hagins, W. A. *Science*, **1977**, *195*, 489. (b) Liu, Y.; Regen, S. L. *J. Am. Chem. Soc*. **1993**, *115*, 708. (c) Nagawa, Y.; Regen, S. L. *J. Am. Chem. Soc*. **1992**, *114*, 1668.

(27) (a) Georgecauld, D.; Desmasez, J. P.; Lapouyade, R.; Babeau, A.; Richard, H.; Winnik, M. *Photochem. Photobiol*. **1980**, *31*, 539−545. (b) Martin, F. J.; MacDonald, R. C. *Biochemistry* **1976**, *15*, 321. (c) Kremer, J. M. H.; Kops-Werkhoven, M. M.; Pathmamanoharan, C.; Gijzemen, O. L. G.; Wiersema, P. H. *Biochim. Biophys. Acta* **1977**, *471*, 177−188.

(28) Benesi, H. A.; Hildebrand, J. H. *J. Am. Chem. Soc*. **1949,** *71*, 2703.

$$Agg_n = n\text{Dimer (or } n\text{Monomer for } mono\text{-SPLs)} \quad (2)$$

$$K = [\text{Di}]^n_{\text{dmpc}}/[\text{Agg}]_{\text{dmpc}} \quad (3)$$

$$\ln[A^n_{\text{di}}/A_{\text{agg}}] = (n-1)\ln[\text{DMPC}] + C \quad (4)$$

In the case of constant [DMPC],

$$\ln A_{\text{agg}} = n \ln[A^{\text{o}}_{\text{aggn}} - A_{\text{aggn}}] + C' \quad (5)$$

The $A^{\text{o}}_{\text{aggn}}$, A_{aggn}, and A_{di} are absorbances of the aggregate added initially, aggregate, and dimer in equilibrium solution, respectively, and they can be obtained simply by spectral subtraction. C and $C'$are constants.

For four SPLs which have relatively low T_c values and are easily accessible to the above method, the plots according to eq 5 give reasonable straight lines as shown in Figure 5. The aggregate sizes, determined by the slopes (n) are 3, 4, 4, and 7 for *bis*-S_4EPC, *bis*-S_4EMPC, *bis*-$_4S_6$EPPC, and *bis*-S_6EPC, respectively, in terms of SPL molecules or 6, 4, 4, and 14, respectively, in terms of numbers of TS per aggregate. For *bis*-S_4EPC and *bis*-S_6EPC, aggregate size measurements were also carried out at different temperatures: at 40 and 45 °C for *bis*-S_6EPC, and 22 and 30 °C for *bis*-S_4EPC. Almost identical results were obtained. Interestingly, the measured aggregate sizes are small although a relatively long range of order is expected in the SPL assemblies. Small aggregate sizes have also been found in other chromophore systems for both H-aggregates (squaraine[29] and semicyanine[30]) and J-aggregates (cyanine dyes[31]). There appears a clear correlation between the extent of the blue-shifts in the absorption spectra of SPL aggregates relative to monomer and the measured aggregate sizes as suggested by the 33, 39, and 45 nm blue-shifts for the tetramer of *mono*-SPLs, the hexamer of *bis*-S_4EPC and the 14mer of *bis*-S_6EPC, respectively. A relatively extended aggregate is anticipated in the monolayers of SFAs and SPLs, which give the largest blue-shifts (47 nm) in absorption. The validity of the aggregate size estimation is strongly supported by a linear relationship of $\ln(A_{\text{di}}{}^3/A_{\text{agg}})$ with [DMPC] according to eq 4 with a slope of 2 for a series of equilibrium samples with the same total concentration of *bis*-S_4EPC vesicles and different concentration of DMPC. The estimated equilibrium constants for the equilibrium between the aggregates and dimers for several SPLs together with the rate constants have been reported previously.[1] In the calculation, the specific partial volume V_m of DMPC was assumed to be identical to that of egg yolk phosphatidycholine vesicles (0.6677 L/mol).[32] The enthalpy and entropy for the deaggregation process over the temperature range of 27−42 °C for *bis*-S_4EPC were found to be ca. 30 kcal/mol and ca. 90 cal/(kmol), respectively. The data below 25 °C for the enthalpy and entropy measurements show a large deviation from the linear plot due to an involvement of the phase transition of DMPC vesicles. Clearly, the aggregation process is enthalpically favored but entropically disfavored. The interaction change involved in the aggregation can be divided into two major components: the hydrophobic interaction and the chromophore−chromophore interaction. Since the "effective" fatty acid chain lengths of *bis*-S_4EPC and DMPC are similar, the hydrophobic interactions in pure *bis*-S_4EPC assemblies, DMPC vesicles, and mixed vesicles of *bis*-S_4EPC and DMPC are expected to show small differences and thus contribute little to the overall change for the aggregation. The primary difference between the aggregate and the dimer in dilute DMPC vesicles is the chromophore−chromophore interaction. One mole of TS in the aggregate is enthalpically 5 kcal more stable than in the dimer. This extra stability can be attributed to the apolar association between the TS chromophores.[33,34] Similar results have also been obtained for azobenzene,[9] squaraine,[29b] and styrylthiophene[23] derivatives. The relatively high stability of these "unit aggregates" compared to the dimers thus suggests that there are attractive noncovalent interactions beyond those in the dimer.

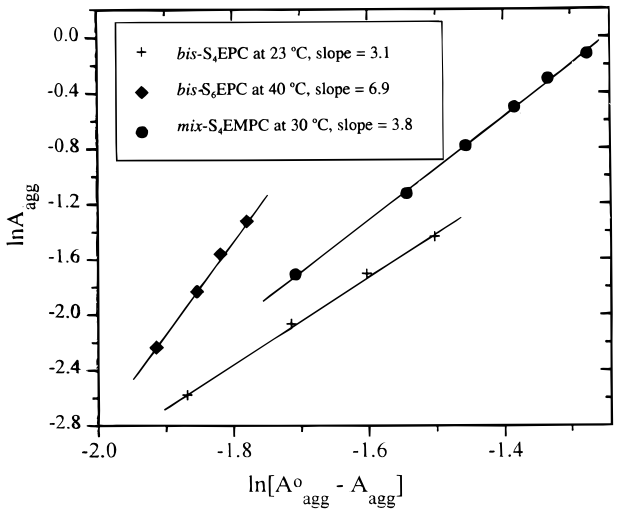

Figure 5. Benesi−Hildebrand plots of ln A_{agg} as a function of ln($A^{\text{o}}_{\text{agg}}$ − A_{agg}) for SPLs in DMPC vesicles.

The deaggregation processes for *bis*-S_4EPC, *bis*-S_4EMPC, and *bis*-S_6EPC assemblies and possibly other SPLs with DMPC or DPPC vesicles at or above T_c values show first-order kinetics for SPLs in each case. For the case of S_6EPC and possibly other SPLs, the deaggregation rates are independent of DMPC concentration. This suggests that the aggregates dissociate slowly (or are extruded into bulk solution) to form dimers or monomers followed by rapid trapping by the matrix of DMPC vesicles.

Induced Circular Dichroism (ICD) Spectra. No CD signals are detected for SPL monomers in organic solvents such as chloroform even though the SPLs are chiral. The reason is apparent since the achiral TS chromophores are relatively far away from the chiral center and the two fatty chains are flexible. In contrast, fresh aqueous dispersions of SPLs prepared by sonication exhibit strong biphasic ICD spectra (Figure 6) with a positive Cotton effect in the long wavelength region and a negative Cotton effect in the short wavelength region for all SPLs (with the exception of S_4EPC which, surprisingly, has a reverse biphasic ICD spectrum). The two strong Cotton effects are associated with two allowed optical transitions for the aggregates. The energy difference between the two transitions is too small to be resolved by absorption spectroscopy. The occurrence of the zero-cross points of the ICD for all SPLs at the λ_{max} of the blue-shifted absorption spectra suggests that the ICD are associated with the exciton band of the H-aggregates (see the Supporting Information). These strongly enhanced ICD are attibuted to the chiral structures of the H-aggregates.[35] Although the blue-shifted absorption spectra of SPL assemblies are independent of preparation techniques and conditions, the

(29) (a) Chen, H.; Law, K. Y.; Whitten, D. G. *J. Am. Chem. Soc*. **1995**, *117*, 7257. (b) Chen, H.; Farahat, M. S.; Law, K. Y.; Perlstein, J.; Whitten, D. G. *J. Am. Chem. Soc.* **1996**, *118*, 2586.

(30) Bohn, P. W. Private communication.

(31) Samha, H.; Whitten, D. G. Unpublished results.

(32) Gennis, R. B. *Biomembrane, Molecular Structure and Function*; Springer-Verlag: Berlin, 1989.

(33) Smithrud, D. B.; Sanford, E. M.; Chao, I.; Ferguson, S. B.; Carcanague, D. R.; Evanseck, J. D.; Houk, K. N.; Diederich, F. *Pure Appl. Chem*. **1990**, *12*, 2227−2236.

(34) Dewey, T. G.; Wilson, P. S.; Turner, D. H. *J. Am. Chem. Soc*. **1978**, *100*, 4550.

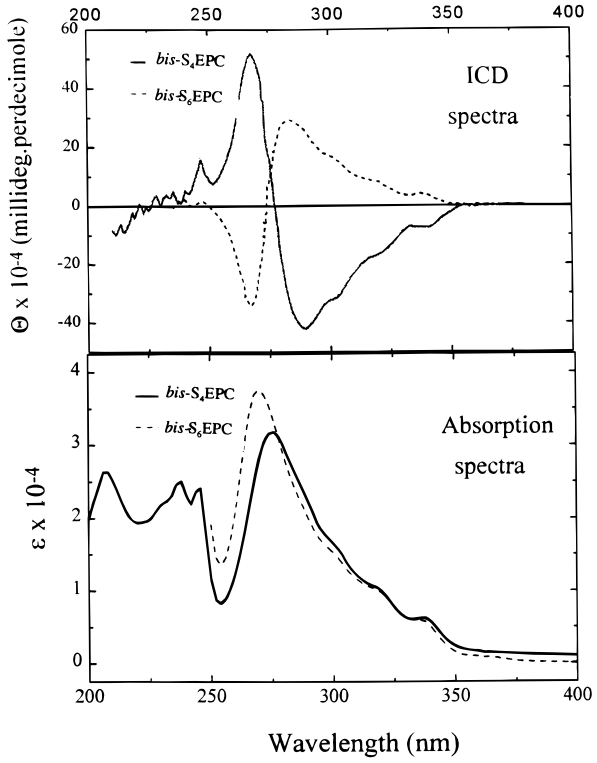

Figure 6. ICD (top) and absorption (bottom) spectra of *bis*-S_4EPC and *bis*-S_6EPC assemblies in water.

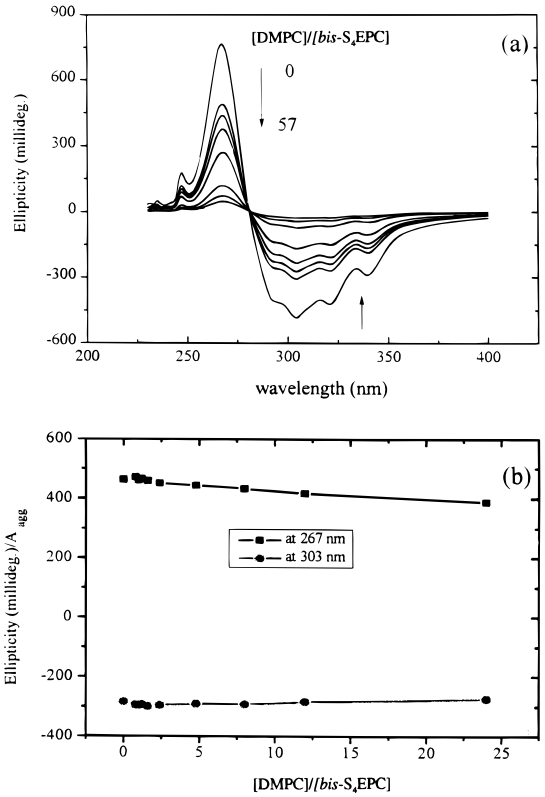

Figure 7. (a) ICD spectra of *bis*-S_4EPC in DMPC vesicles. All of the samples contain identical concentration of DMPC and different concentration of *bis*-S_4EPC. (b) ICD intensity normalized by aggregate-absorbance versus the dilution ratio of [DMPC]/[*bis*-S_4EPC].

apparent molecular ellipticity for the ICD is subject to a change under different preparation conditions, indicative of coexistence of two interconvertible enantioners in the solution. It is reasonable to suggest that both the chirality of the head group and the alignment of stilbenes in the aggregates determine the ICD spectra. The dimer for SPLs and monomer for SFAs or *mono*-SPLs in an excess of chiral hosts of DPPC or DMPC vesicles exhibit no detectible ICD signals. The mixtures of aggregates and dimers (or monomers) in SPLs moderately diluted with DMPC or DPPC give ICDs identical to those for pure SPL aqueous dispersions. Figure 7 shows the ICD spectra and the aggregate-absorbance-normalized ICD intensity as a function of dilution ratio for S_4EPC solubilized in DMPC vesicles. The common zero-cross points for ICD spectra for all of the samples with different dilution ratio and the independence of the absorbance-corrected ellipticity on the dilution ratio clearly indicate that the aggregates in DPPC or DMPC vesicles are the same as those in pure SPL assemblies and only the aggregates and dimers (or monomers) in the DPPC or DMPC vesicles are involved in the solution. The temperature-induced phase transition of SPL assemblies in water has little effect on the ICD spectra except a decrease in intensity. This is consistent with small aggregates of relatively high stability, which remain unperturbed through the melting process of the fatty acid chains.

Steady State Photolysis. We have observed that the aggregation in the monolayers[2] and bilayer assemblies[44] of TS derivatives shuts down the *trans*−*cis* photoisomerization observed for isolated TS in solution. Irradiation of pure aqueous solutions of a number of *trans*-SPLs results in a slow, but detectable photoreaction, which is monitored by UV−vis absorption, fluorescence, and ICD spectra at regular intervals during the photolysis. Similar results are obtained for 280 and 320 nm excitation wavelengths. Bleaching of the main aggregate absorption band (at or near 270 nm) was observed in all cases. However, the extent of the bleaching, as well as the shape of the spectra after photolysis, was sample dependent. ICD spectra showed only a decrease in intensity consistent with disappearance of the optically active chromophore in the samples as shown in Figure 8. The shape of the ICD spectra remained constant throughout the experiments. Isosbestic points are observed for both absorption and ICD spectra, which suggests a clear conversion from the aggregates to photoproduct(s). The length of time required to achieve certain extent of bleaching for the aggregate absorption band at ca. 270 nm was used to provide a qualitative measure of relative bleaching efficiencies (180, 32, 20 and 4.5 min of irradiation are required for 25% decrease in the peak absorbance for *bis*-S_{10}EPC, *bis*-S_4EPC, *bis*-$_4S_4$EPC and *bis*-$_4S_6$EPC, respectively, keeping all experimental conditions constant). True bleaching efficiencies could not be obtained due to the appearance of a new light absorbing species in the spectral region associated with the starting material. The processes causing the observed spectral changes for SPLs is far less efficient than the *trans*−*cis* photoisomerization process for TS in fluid solutions. The extremely low bleaching efficiency of *bis*-S_{10}EPC assemblies is consistent with a stable and uniform aggregate. Some evidence from both spectroscopic and ^{1}H NMR data of one major product resulting from irradiation at 280 nm of SPL assemblies in water suggests occurrence of a photodimerization.[36] Such a photodimerization of TS as a major process has also been observed for bilayer asssemblies of other TS-derivatized amphiphiles in water, where similar aggregates were formed.[44] In another case, a crystalline TS derivative has been found to display excimer emission and undergoes photocyclization to generate a mirror symmetric dimer.[43] The unambiguous identification of the photoproduct(s) and the involved mechanism for the aggregates is a subject of further investigation.

(35) (a) Cassim, J. Y. *Biophys. J.* **1992**, *63*, 1432−1442. (b) Person, R. V.; Peterson, B. R.; Lighter, D. A. *J. Am. Chem. Soc.* **1994**, *116*, 42−59. (c) Wu, S.; El-Sayed, M. A. *Biophys. J.* **1991**, *60*, 190−197. (d) Ebrey, T. G.; Becker, B.; Mao, B.; Kilbride, P. *J. Mol. Biol.* **1977**, *112*, 377−397.

(36) Farahat, M. Unpublished results.

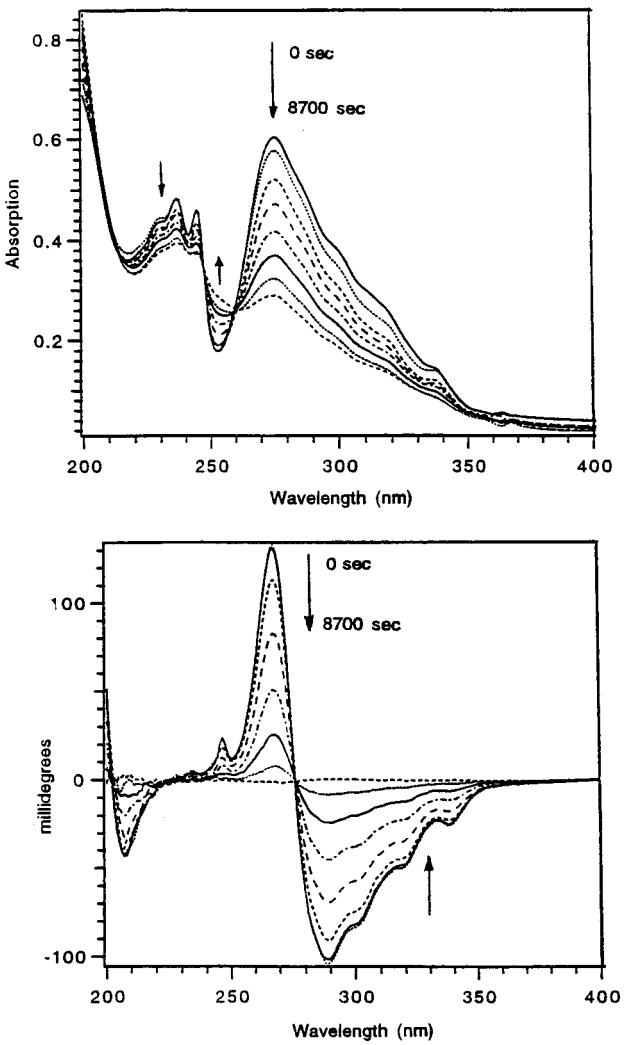

Figure 8. Absorption (top) and ICD (bottom) spectra of *bis*-S_4EPC assemblies in water at different stages of irradiation at 280 nm.

The fluorescence spectra for the irradiated samples showed more variations in shape and intensity between different samples compared to the corresponding absorption spectra. The major effect of photolysis was the decrease in intensity of the fluorescing species. The extent of this reduction was highly dependent on the structure of the SPLs used. Extended photolysis of SPL assemblies in water leads to appearance of a new structured fluorescence band near 350 nm that resembles that of derivatized TS in organic solution (see the Supporting Information). This fluorescence is attributed to unaggregated TS chromophores that remain after a large population of their neighboring moieties have undergone photodimerization and cease to contribute to excitonic interactions. Due to the rigidity of their environment, these isolated TS chromophores are not expected to undergo *trans*−*cis* isomerization and to show a high fluorescence efficiency.

Monolayers. We have examined an array of amphiphilic TS fatty acid derivatives and *trans,trans*-1,4-diphenyl-1,3-butadiene and *trans,trans,trans*-1,6-diphenyl-1,3,5-hexatriene derivatives in supported assemblies[2,8] where H-aggregation with a characteristic blue-shifted absorption and a red-shifted fluorescence is observed. In several cases, only H-aggregates can be detected, even for LB films of mixtures of the aromatics diluted with a large excess of fatty acid host. Reflectance spectroscopic study of SFA monolayers at the water−air interface provides some new insights into the H-aggregation behaviors of these aromatics. As shown in Figure 9 (inset), a sharp π-area isotherm for $_4S_4A$ monolayer was obtained, and

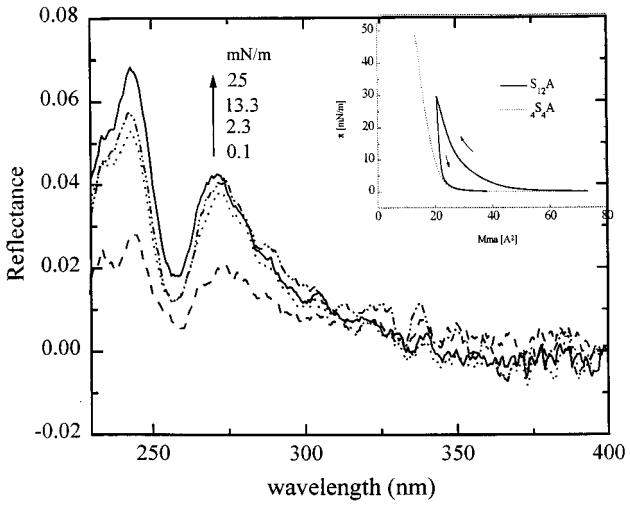

Figure 9. Reflectance spectra of $_4S_4A$ monolayer at the air−water interface at difference surface pressures. Inset: Surface pressure−area isotherm of $_4S_4A$ monolayer and hysteresis of $S_{12}A$ monolayer.

the molecular area is estimated to be ca. 22 Å^2, consistent with the reported data[1] for the first compression of $_4S_4A$. In contrast, the π-area isotherm for the first compression is broad for $S_{12}A$ monolayer, but sharp for the first decompression process. In contrast with the monomeric absorption spectrum of TS in solution, the reflectance spectrum of the $_4S_4A$ monolayer at the water−air interface shows blue-shifts similar to the absorption spectra of supported LB films of SFAs and bilayer assemblies of SPLs. The reflectance spectra change little except in intensity from very low pressures prior to compression to relatively high pressure, indicating that the aggregates are preformed even in the expanded liquid or gaseous state. Dilution of $_4S_4A$ monolayer with stearic acid (SA) up to SA/$_4S_4A$ = 4/1 shows little effect on H-aggregate formation as indicated by the persistence of similar H-aggregate reflectance spectra. Similar behavior is observed for the $_4S_6A$ monolayer. The fact that the H-aggregates are the only observed aggregation form for TS and other diphenyl polyene derivatives in supported films and monolayers at the air/water interface indicates the high stability of H-aggregated forms. Related studies for some squaraine derivatives[37] showed similar results in that the H-aggregates of squaraine also preform without compression at the water−air interface.

Reflectance spectra of $_4S_4A$ and $_4S_6A$ monolayers consist of two major peaks at 268 and 240 nm, which correspond to two transition dipoles, one along the long axis of TS and the other perpendicular to the long axis, repectively.[37] Strikingly different reflectance spectra were obtained for $S_{12}A$ and $S_{10}A$ monolayers, which shows only one peak at 240 nm. The absence of the peak at 268 nm for $S_{12}A$ and $S_{10}A$ suggests that the chromophores are oriented perpendicular to the water surface, since the incident light used for the reflectance measurement is normal to the water surface. The presence of both absorption peaks for $_4S_4A$ and $_4S_6A$ indicates that the stilbene chromophore is tilted to some extent from the water surface normal.

Aggregate Structure. Monolayer and bilayer assemblies are highly ordered and can be considered to be two-dimensional lattices with some long-range order. Monte Carlo cooling methods have previously been used to determine the apparent global and nearby local minima structures for monolayers.[38] Applying these procedures,[38] we have found[1b] that the lowest energy structures, which show closest agreement with the

(37) Chen, H.; Liang, K. L. Song, X.; Samha, H.; Law, K. Y.; Perlstein, J.; Whitten, D. G. In *Micelles, Microemulsions, and Monolayers. Science and Technology*; Shah, D., Ed.; Marcel Dekker, Inc. New York, 1995, in press.

limiting area/molecule and the predicted exciton splitting, are the global minimum glide or herringbone arrangement for $_4S_6A$ and the first local minimum for S_4A. While we have not yet been able to calculate structures (monolayer or bilayer) for the phospholipids containing two SFA units, the similarity of spectra and photophysics[2] suggests similar structures for the aggregates of both SFA's and phospholipids in the monolayer films and bilayer assemblies. Thus, we have proposed that a glide layer structure is the extended arrangement for the TS chromophores in the aggregates of the SPLs in water. The strong biphasic ICD for the aggregates of the SPLs indicates that the aggregate structures are chiral with two different TS chromophores per unit cell in the two-dimensional lattice of the glide layer. While the infinite glide or herringbone lattice is not chiral, the smaller units within the layer structure, most notably the "pinwheel" tetramer or other cyclic structures, are chiral (see ref 1b). Taking together the likelihood of a glide structure as the arrangement of an extended aggregate and the measured aggregation number, we propose a "pinwheel" structure as the most likely arrangement for the smallest "unit" aggregates. These structures, with two different stilbenes in each "unit" aggregate, are chiral and account nicely for the observed biphasic ICD spectra associated with the aggregates. These structures are also attractive in that they maximize the number of "T" interactions (face-to-edge or $\sigma-\pi$ interaction) which have been demonstrated to stablize the dimers of benzene[39] and related aromatics.[40] The favored structure for the benzene dimer from both theory and experiment is a "T" arrangement with stabilizing edge−face interaction. Our studies for other aromatic systems including azobenzene, styrylthiophene, and tolan as well as squaraine also suggest that the "pinwheel" units may be a general supramolecular energy minimum for a variety of aromatics and conjugated compounds such as diphenylbutadienes and diphenylhexatrienes, since they give very similar aggregation under similar conditions. An X-ray diffraction study of several weakly amphiphilic TS deirvatives provides support for the pinwheel or unit aggregate as a key component in the formation of crystals or extended aggregates.[41]

Summary

Blue-shifted absorption and red-shifted fluorescence spectra similar to those in monolayers and LB films of SFAs were observed for SPL assemblies in water in contrast to normal "monomeric" absorption and fluorescence spectra for SFAs and SPLs in organic solvents. The blue-shifted spectra are attributed to the formation of H-aggregates, in which the transition dipole moments of the TS chromophores are aligned in a general head-to-head arrangement. The complicated fluorescence of the SPLs in water is believed to result from the heterogeneity of the assemblies and possible energy transfer between aggregates and excimers (or a geometrical change in excited state of the aggregates which results in the formation of the excimer). Evaluation of the equilibrium between the aggregates and dimers (or monomers) of SPLs in the matrix of DPPC or DMPC vesicles allowed determination of aggregate numbers and thermodynamic parameters associated with the aggregation process. The measured aggregate sizes show a good correlation with the observed blue-shifts in absorption for several SPLs. The strong biphasic ICD spectra associated with the aggregates indicated the chiral nature of the aggregates in which there are two different stilbenes in the unit aggregate. Monte Carlo cooling simulation results[1] indicate that a glide layer or herringbone structure is the most probable structures for an extended array of SFAs in a monolayers. Taking into account the measured aggregate sizes, the chiral nature of the aggregates, and the spectral similarity of SPL assemblies in water to SFA, monolayers, as well as the simulated structures, small cyclic chiral "pinwheel" structures are proposed as likely structures of the H-aggregates. Extended aggregates can be fairly described as a mosaic of these small aggregate units. The structures are reasonable in view of the likely maximization of weakly $\sigma-\pi$ (face−edge) attractive forces and minimization of $\pi-\pi$ repulsions between the closely packed stilbene chromophores.[42]

Acknowledgment. We are grateful to the National Science Foundation (Grant CHE-9211586) for support of this research.

Supporting Information Available: Various spectra (6 pages). See any current masthead page for ordering and Internet access instructions.

JA972292I

(38) (a) Chen, H.; Law, K. Y.; Perlstein, J.; Whitten, D. G. *J. Am. Chem. Soc*. **1995**, *117*, 7257. (b) Perlstein, J. *J. Am. Chem. Soc.* **1994**, *116*, 455. (c) Perlstein, J. *J. Am. Chem. Soc*. **1994**, *116*, 11420.

(39) (a) Arunan, E.; Gutowsky, H. S. *J. Chem. Phys*. **1993**, *98*, 4294. (b) Hall, D.; Williams, D. F. *Acta Crystallogr*. **1975**, *A31*, 56.

(40) (a) Schweitzer, B. A.; Kool, E. T. *J. Am. Chem. Soc*. **1995**, *117*, 1863. (b) Winnik, F. M. *Chem. Rev.* **1993**, *93*, 587.

(41) Vaday, S.; Geiger, H. C.; Perlstein, J.; Whitten, D. G. *J. Phys. Chem*. **1997**, *101*, 321.

(42) (a) Linse, P. *J. Am. Chem. Soc*. **1993**, *115*, 8793. (b) Hunter, C. A.; Saunders, J. K. M. *J. Am. Chem. Soc*. **1990**, *112*, 5525−5534. (c) Jorgenson, W. L.; Severance, D. L. *J. Am. Chem. Soc*. **1990**, *112*, 4768−4774. (d) Shi, X.; Bartell, L. S. *J. Phys. Chem*. **1988**, *92*, 5667−5673. (e) Pawliszyn, J.; Szczesniak, M. M.; Scheiner, S. *J. Phys. Chem*. **1984**, *88*, 1726−1730.

(43) Cohen, M. D.; Green, B. S.; Ludmer, Z.; Schmidt, G. M. *Chem. Phys. Lett.* **1970**, *7*, 486.

(44) Shimomura, M.; Hashimoto, H.; Kunitake, T. *Langmuir* **1989**, *5*, 174.

(45) Agbaria, R. A.; Roberts, E.; Warner, I. M. *J. Phys. Chem*. **1995**, *99*, 10056.